

Vibrational and electronic circular dichroism spectroscopies and DFT calculations for the assignment of the absolute configuration
of hydroxy substituted 2-tetralols

Sergio Abbate, France Lebon, Giovanna Longhi, Carlo F. Morelli, Daniela Ubiali and Giovanna Speranza

Contents:

Fig.SI-1 Contour plot of the 2D potential surface for (*R*)-1-tetralol (**1a**) against dihedral angles $H_2C_2C_1O$ (τ) and C_9C_1OH (φ) (A) and for (*R*)-1-aminotetralin (**1b**) against angles $H_2C_2C_1N$ (τ) and C_9C_1NH (φ) (B) at the B3LYP/6-31G(d,p) level.

Fig.SI-2 Contour plot of the 2D potential surface for (*R*)-2-tetralol (**2a**) against dihedral angles $H_1C_1C_2O$ (τ) (a) and C_1C_2OH (φ) at the B3LYP/6-31G(d,p) level.

Fig.SI-3: Contour plot of the 2D potential surface for (*R*)-5-hydroxy-2-tetralol (**2b**) against dihedral angles $H_1C_1C_2O$ (τ) and C_1C_2OH (φ) with $C_{10}C_5O_5H$ (χ) at 180° (A) and 0° (B) at the B3LYP/6-31G(d,p) level.

Fig.SI-4: Contour plot of the 2D potential surface for (*R*)-8-hydroxy-2-tetralol (**2c**) against dihedral angles $H_1C_1C_2O$ (τ) and C_1C_2OH (φ) with $C_9C_8O_8H$ (χ) at 180° (A) and 0° (B) at the B3LYP/6-31G(d,p) level.

Fig. SI-5: B3PW91/TZ2P optimized structures and relative energies (kcal/mol) for (*R*)-1-tetralol (**1a**) in vacuo

Fig.SI-6: B3PW91/TZ2P optimized structures and relative energies (kcal/mol) for (*R*)-2-tetralol (**2a**) in vacuo.

Fig.SI-7: B3PW91/TZ2P optimized structures and relative energies (kcal/mol) for (*R*)-5-hydroxy-2-tetralol (**2b**) in vacuo.

Fig.SI-8: B3PW91/TZ2P optimized structures and relative energies (kcal/mol) for (*R*)-8-hydroxy-2-tetralol (**2c**) in vacuo.

Fig.SI-9: B3PW91/TZ2P optimized structures and relative energies (kcal/mol) for (*R*)-1-aminotetralin (**1b**) in vacuo.

FigSI-10a: Calculated IR (top) and VCD (bottom) spectra of stable conformers of (*R*)-(-)-1-tetralol (**1a**) in vacuo (left) and in chloroform (right) with IEF-PCM method (B3PW91/TZ2P). FigSI-10b: Calculated IR (top) and VCD (bottom) spectra of stable conformers of (*R*)-(-)-1-tetralol (**1a**) in methanol with IEF-PCM method (B3PW91/TZ2P).

FigSI-11a: Calculated IR (top) and VCD (bottom) spectra of stable conformers of (*R*)-(+)-2-tetralol (**2a**) in vacuo (left) and in chloroform (right) with IEF-PCM method (B3PW91/TZ2P). FigSI-11b: Calculated IR (top) and VCD (bottom) spectra of stable conformers of (*R*)-(+)-2-tetralol (**2a**) in methanol (right) with IEF-PCM method (B3PW91/TZ2P).

FigSI-12: Calculated IR (top) and VCD (bottom) spectra of stable conformers of (*R*)-(+)-5-hydroxy-2-tetralol (**2b**) in vacuo (left) and in methanol (right) with IEF-PCM method (B3PW91/TZ2P).

FigSI-13: Calculated IR (top) and VCD (bottom) spectra of stable conformers of (*R*)-(+)-8-hydroxy-2-tetralol (**2c**) in vacuo (left) and in methanol (right) with IEF-PCM method (B3PW91/TZ2P).

Fig.SI-14: Calculated IR (top) and VCD (bottom) spectra of stable conformers of (*R*)-1-aminotetralin (**1b**) in *vacuo* (B3PW91/TZ2P).

Fig. SI-15: TDDFT calculated absorption and ECD spectra of (*R*)-1-tetralol (**1a**) on the left and (*R*)-2-tetralol (**2a**) on the right with stable conformers (top) and weighted sum (bottom) using B3LYP-TZVP

Fig. SI-16: TDDFT calculated absorption and ECD spectra of (*R*)-5-hydroxy-2-tetralol (**2b**) on the left and (*R*)-8-hydroxy-2-tetralol (**2c**) on the right with stable conformers (top) and weighted sum (bottom) using B3LYP-TZVP

Fig. SI-17: Calculated absorption and ECD spectra of (*R*)-1-aminotetralin (**1b**) with stable conformers (top) and weighted sum (bottom) using B3LYP-TZVP.

Fig.SI-18: Experimental (solid line) and calculated (dashed line) UV absorption spectra of (*R*)-1-tetralol (**A**), (*R*)-2-tetralol (**B**); (*R*)-5-hydroxy-2-tetralol (**C**), (*R*)-8-hydroxy-2-tetralol (**D**) and (*R*)-1-aminotetralin (**E**)

Table SI-1: Calculated conformer population factors (%) based on ΔG for (*R*)-1-tetralol (**1a**) and (*R*)-2-tetralol (**2a**) using B3PW91/TZ2P and B97D/TZ2P levels of theory within the PCM-CHCl₃ model.

Fig. SI-19a: Experimental and calculated (weighted sum) IR (top) and VCD (bottom) spectra of (*R*)-1-tetralol (left panels) (**1a**) and (*R*)-2-tetralol (right panels) (**2a**) with B3PW91 (pink) and B97D (green) functionals with IEF-PCM (CHCl₃) method. The

calculated IR and VCD spectra with B3PW91 functional using the population factor extracted from B97D calculations have been presented in blu.

Fig. 19b. Calculated IR (top) and VCD (bottom) spectra for the six stable conformers of (*R*)-1-tetralol (left panels) (**1a**) and (*R*)-2-tetralol (right panels) (**2a**) on the basis of B97D/TZ2P level of theory for the PCM-CHCl₃ model.

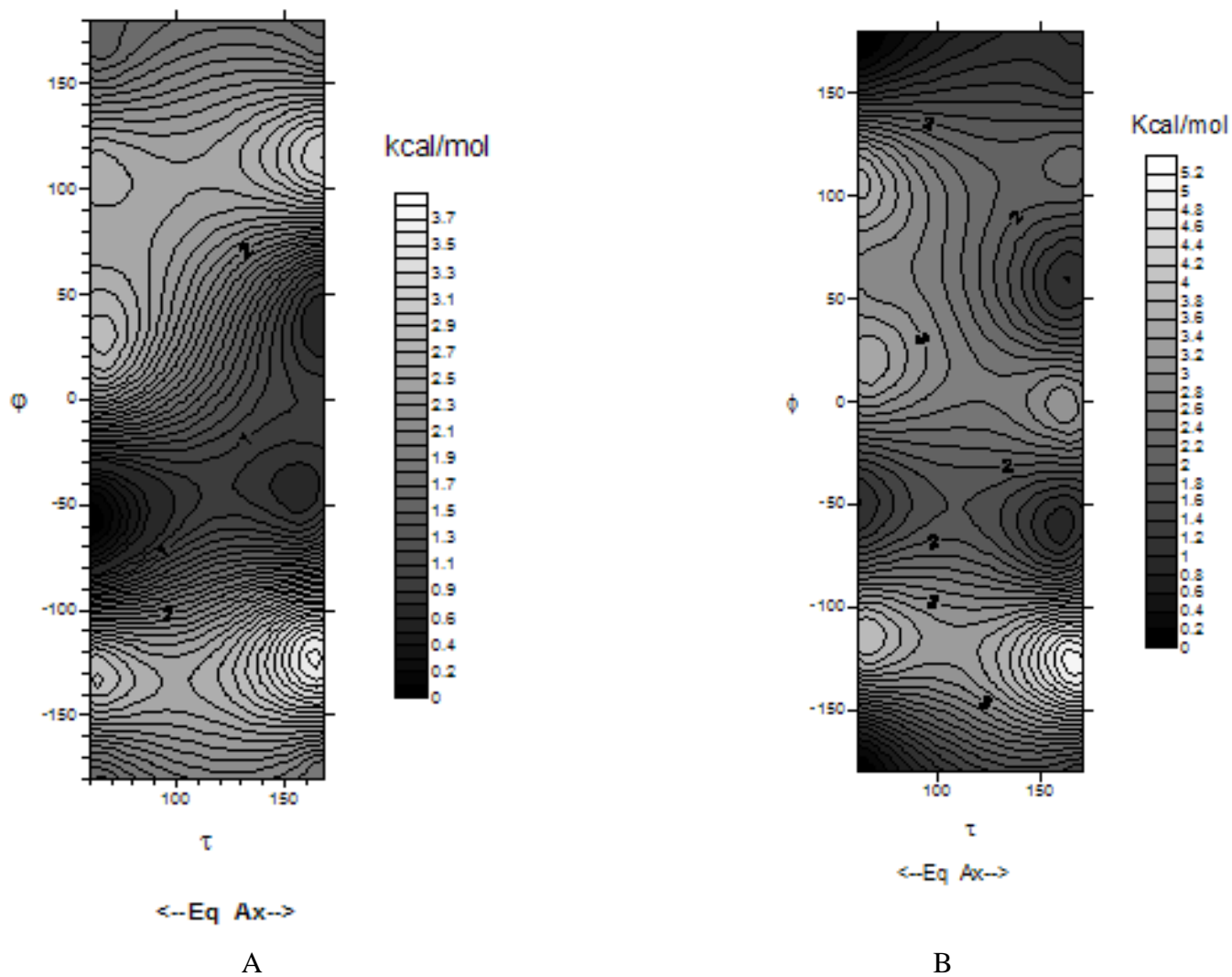


Fig.SI-1 Contour plot of the 2D potential surface for (*R*)-1-tetralol (**1a**) against dihedral angles $\text{H}_2\text{C}_2\text{C}_1\text{O}$ (τ) and $\text{C}_9\text{C}_1\text{OH}$ (ϕ) (A) and for (*R*)-1-aminotetralin (**1b**) against angles $\text{H}_2\text{C}_2\text{C}_1\text{N}$ (τ) and $\text{C}_9\text{C}_1\text{NH}$ (ϕ) (B) at the B3LYP/6-31G(d,p) level.

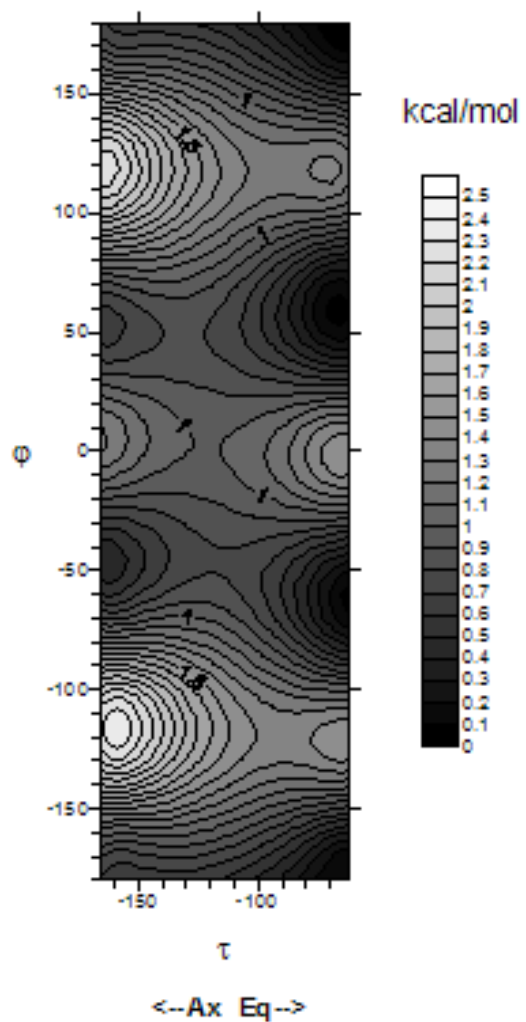


Fig.SI-2 Contour plot of the 2D potential surface for (*R*)-2-tetralol (**2a**) against dihedral angles $H_1C_1C_2O$ (τ) and C_1C_2OH (ϕ) at the B3LYP/6-31G(d,p) level.

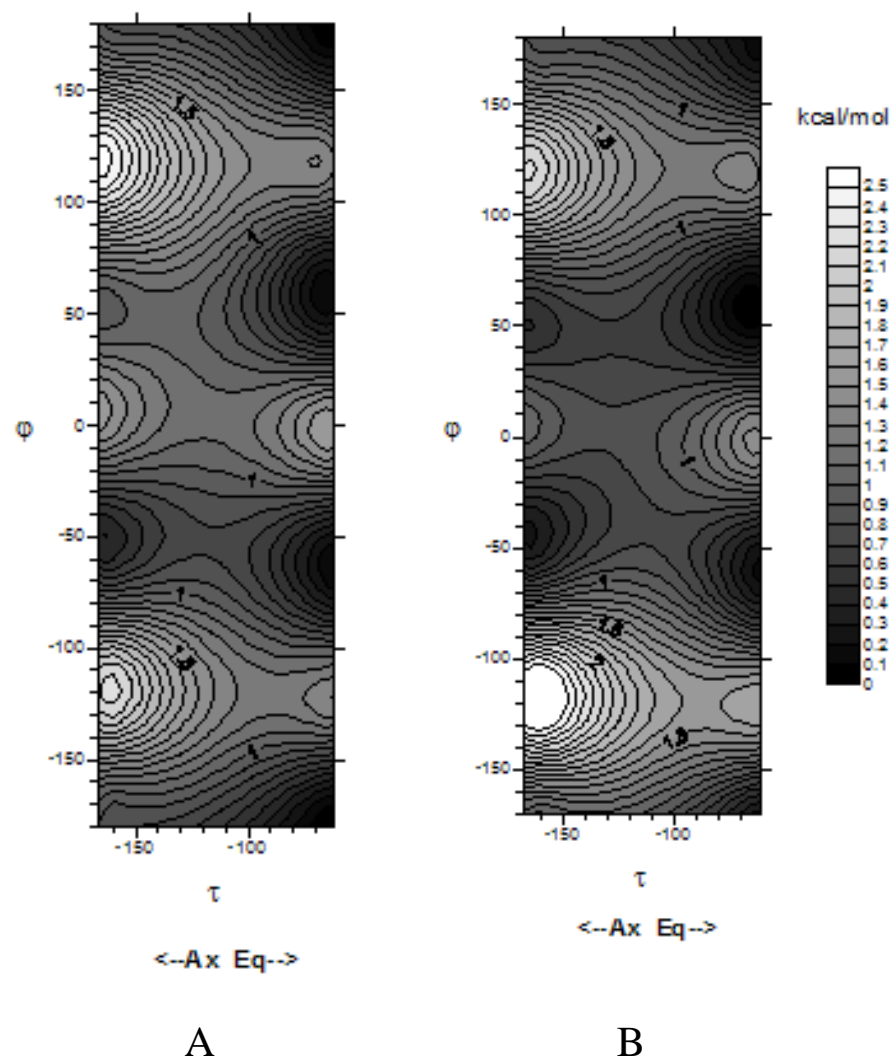


Fig.SI-3: Contour plot of the 2D potential surface for *(R)*-5-hydroxy-2-tetralol (**2b**) against dihedral angles $\text{H}_1\text{C}_1\text{C}_2\text{O}$ (τ) and $\text{C}_1\text{C}_2\text{OH}$ (ϕ) with $\text{C}_{10}\text{C}_5\text{O}_5\text{H}$ (χ) at 180° (A) and 0° (B) at the B3LYP/6-31G(d,p) level.

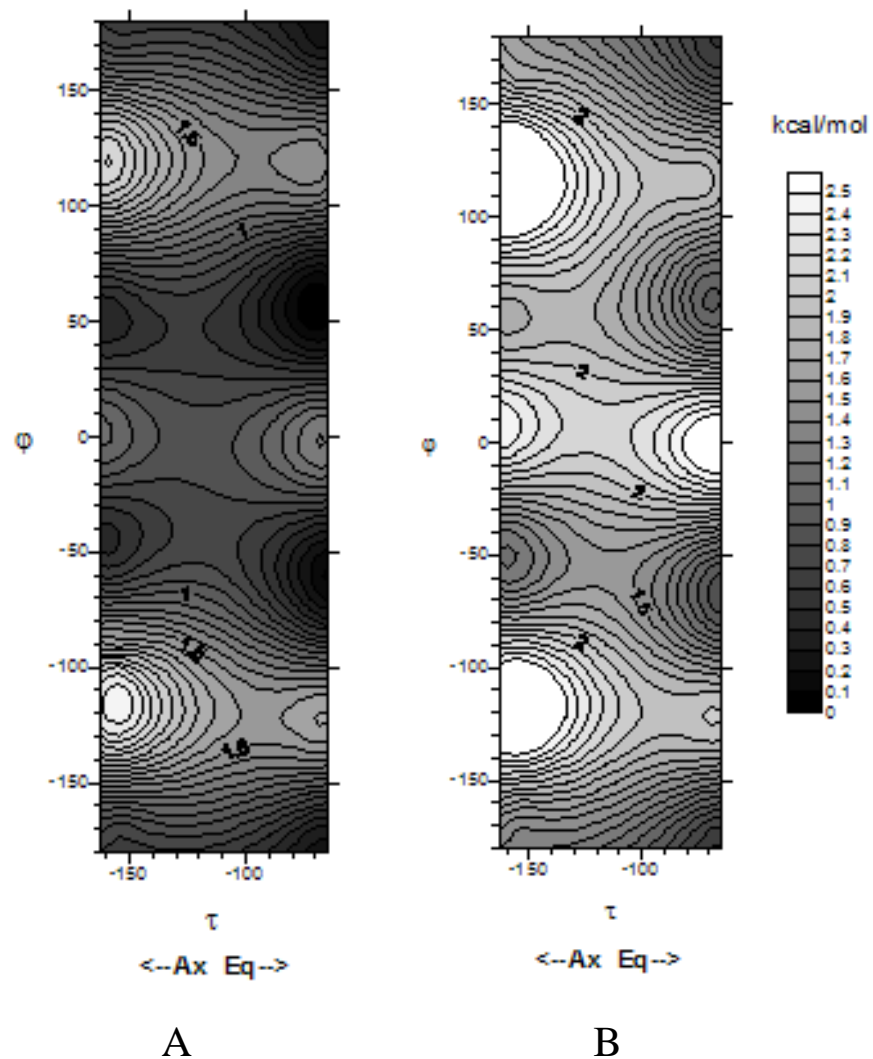
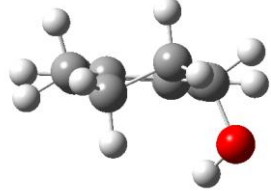
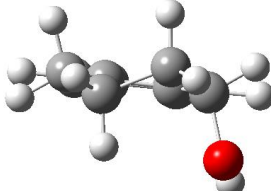
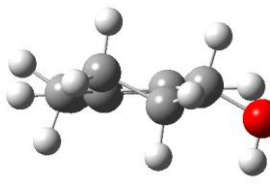
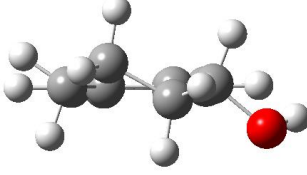
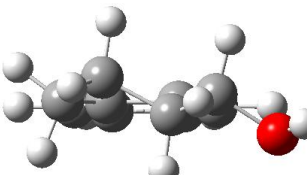
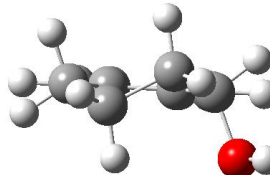


Fig.SI-4: Contour plot of the 2D potential surface for (*R*)-8-hydroxy-2-tetralol (**2c**) against dihedral angles $H_1C_1C_2O$ (τ) and C_1C_2OH (ϕ) with $C_9C_8O_8H$ (χ) at 180° (A) and 0° (B) at the B3LYP/6-31G(d,p) level.

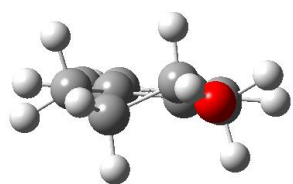
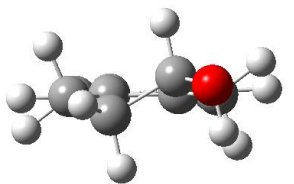
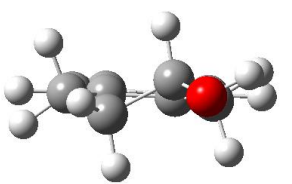
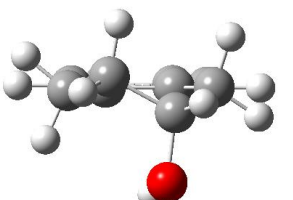
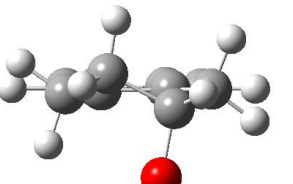
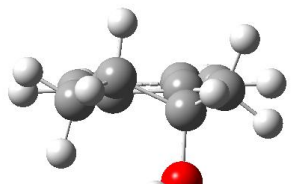
Fig. SI-5: B3PW91/TZ2P optimized structures and relative free energies (kcal/mol) for (*R*)-1-tetralol in *vacuo* (**1a**).

	A		B		C
0 (PCM-MeOD:0; PCM-CHCl ₃ :0.02)		+0.29 (PCM-MeOD:0.29; PCM-CHCl ₃ :0)		+0.62 (PCM-MeOD:0.02; PCM-CHCl ₃ :0.07)	
	D		E		F
+1.32 (PCM-MeOD:1.51; PCM-CHCl ₃ :0.63)		+1.44 (PCM-MeOD:0.95; PCM-CHCl ₃ :0.61)		+1.54 (PCM-MeOD:1.00; PCM-CHCl ₃ : 0.69)	

<i>Vacuo</i>	A	B	C	D	E	F
H ₂ C ₂ C ₁ O*	161	165	61	67	65	166
C ₉ C ₁ OH*	-33	33	-58	61	172	174
C ₁ C ₉ C ₁₀ C ₄ *	4	5	-2	-2	-5	2
C ₂ C ₁ C ₉ C ₁₀ *	-17	-21	19	15	22	-17
C ₉ C ₁₀ C ₄ C ₃ *	-20	-18	17	20	17	-17
C ₄ C ₃ C ₂ C ₁ *	-63	-63	64	64	64	-64
C ₁₀ C ₄ C ₃ C ₂ *	48	46	-47	-49	-46	48
C ₃ C ₂ C ₁ C ₉ *	46	49	-49	-45	-51	47
ΔE (kcal/mol)	0.17	0	0.13	1.90	1.28	1.31
pop (%)	27	36	29	1	4	4
ΔG (kcal/mol)	0	0.29	0.62	1.32	1.44	1.54
Pop.(%)	45	28	16	5	4	3

* in degrees

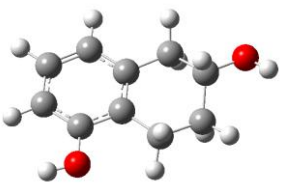
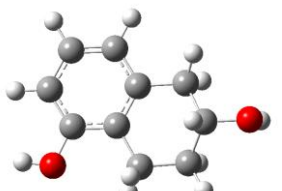
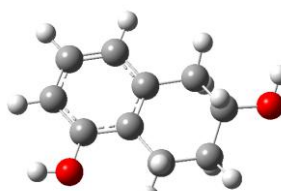
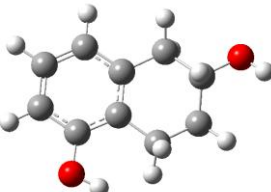
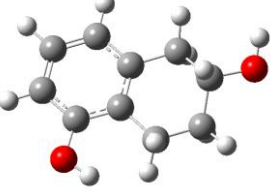
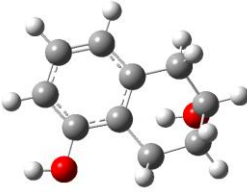
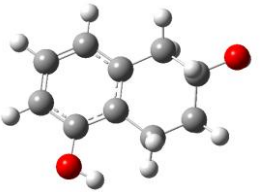

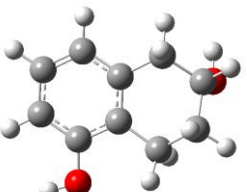
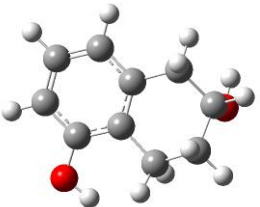
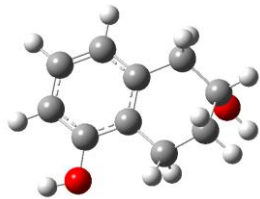
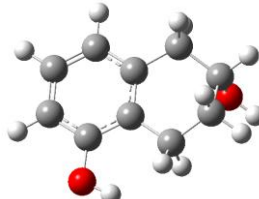
Fig.SI-6: B3PW91/TZ2P optimized structures and relative energies (kcal/mol) for (*R*)-2-tetralol in *vacuo* (**2a**).

	A		B		C
0 (PCM-MeOD:0; PCM-CHCl ₃ :0)		+0.094 (PCM-MeOD:0.15; PCM-CHCl ₃ :0.16)		+0.103 (PCM-MeOD:0.14; PCM-CHCl ₃ :0.12)	
	D		E		F
+0.681 (PCM-MeOD:0.38; PCM-CHCl ₃ :0.90)		+0.779 (PCM-MeOD:0.84; PCM-CHCl ₃ :0.85)		+1.01 (PCM-MeOD:0.98; PCM-CHCl ₃ :0.97)	

<i>Vacuo</i>	A	B	C	D	E	F
H ₁ C ₁ C ₂ O*	-66	-62	-68	-165	-164	-158
C ₁ C ₂ OH*	179	-62	59	-48	51	-178
C ₁ C ₉ C ₁₀ C ₄ *	3	3	4	-4	-4	-4
C ₂ C ₁ C ₉ C ₁₀ *	-19	-18	-20	22	17	15
C ₉ C ₁₀ C ₄ C ₃ *	-18	-18	-17	15	20	22
C ₄ C ₃ C ₂ C ₁ *	-64	-63	-64	62	61	61
C ₁₀ C ₄ C ₃ C ₂ *	48	47	47	-44	-48	-50
C ₃ C ₂ C ₁ C ₉ *	48	48	50	-50	-45	-42
ΔE (kcal/mol)	0	0.15	0.14	0.32	0.66	0.92
pop (%)	27	21	21	16	9	6
ΔG (kcal/mol)	0	0.09	0.10	0.68	0.77	1.00
Pop.(%)	29	25	24	9	8	5

* in degrees

Fig.SI-7: B3PW91/TZ2P optimized structures and relative energies (kcal/mol) for (*R*)-5-hydroxy-2-tetralol in *vacuo* (**2b**).

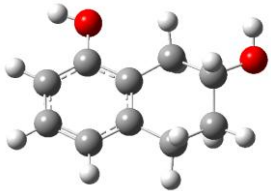
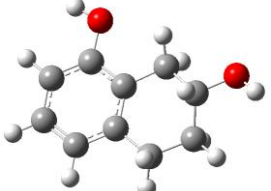
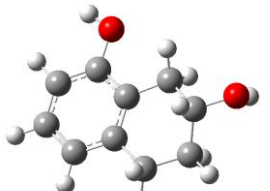
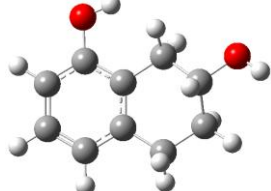
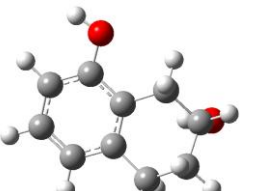
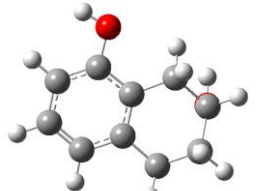
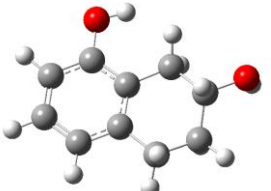
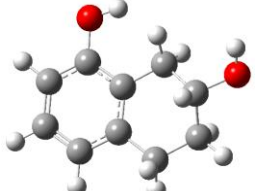
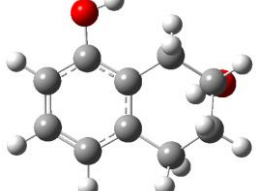
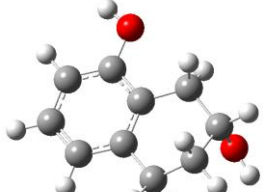
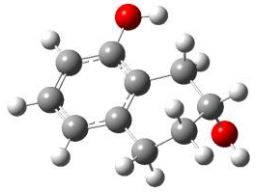
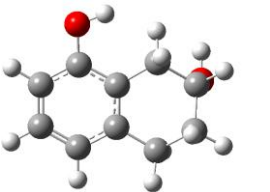
	A		B		C
0 (PCM:0)		+0.19 (PCM:0.23)		+0.20 (PCM:0.18)	
	D		E		F
+0.61 (PCM:0.41)		+0.64 (PCM:0.40)		+0.65 (PCM:0.40)	
	G		H		I
+0.76 (PCM:0.56)		+0.91 (PCM:0.62)		+0.92 (PCM:1.06)	
	J		K		L
+0.98 (PCM:0.95)		+1.14 (PCM:1.18)		+1.62 (PCM:1.30)	

<i>Vacuo</i>	A	B	C	D	E	F
H ₁ C ₁ C ₂ O*	-65	-62	-67	-65	-67	-165
C ₁ C ₂ OH*	-180	-63	59	178	59	-52
C ₁₀ C ₅ O ₅ H*	-179	-179	-179	0	0.2	179
ΔE (kcal/mol)	0	0.17	0.18	0.61	0.55	0.28
pop (%)	19	14	14	7	7	12
ΔG (kcal/mol)	0	0.19	0.20	0.61	0.64	0.65
Pop.(%)	22	16	16	8	7	7

<i>Vacuo</i>	G	H	I	J	K	L
H ₁ C ₁ C ₂ O*	-62	-167	-166	-166	-160	-161
C ₁ C ₂ OH*	-59	-44	51	49	-175	179
C ₁₀ C ₅ O ₅ H*	0.5	0	180	-2	180	-2
ΔE (kcal/mol)	0.67	0.60	0.87	0.91	1-02	1.50
pop (%)	6	7	4	4	3	2
ΔG (kcal/mol)	0.76	0.91	0.92	0.98	1.14	1.62
Pop.(%)	6	5	5	4	3	1

* in degrees

Fig.SI-8: B3PW91/TZ2P optimized structures and relative energies (kcal/mol) for (*R*)-8-hydroxy-2-tetralol in *vacuo* (**2c**).

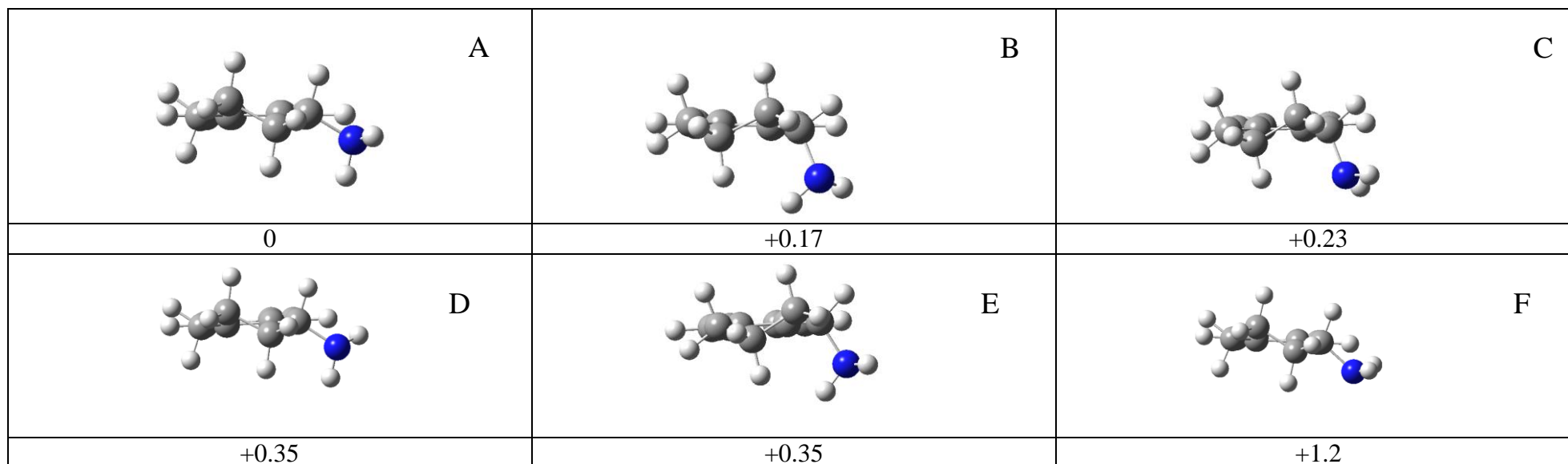
	A		B		C
0 (PCM:0.046)		+0.057 (PCM:0.10)		+0.12 (PCM:0.14)	
	D		E		F
+0.18 (PCM:0)		+0.50 (PCM:0.36)		+0.53 (PCM:0.64)	
	G		H		I
+0.58 (PCM:0.38)		+0.60 (PCM:0.47)		+0.92 (PCM:0.62)	
	J		K		L
+1.02 (PCM:0.98)		+1.37 (PCM:1.21)		+1.50 (PCM:1.45)	

<i>Vacuo</i>	A	B	C	D	E	F
H ₁ C ₁ C ₂ O*	-70	-69	-66	-69	-161	-162
C ₁ C ₂ OH*	56	178	-59	179	-46	49
C ₉ C ₈ O ₈ H*	-180	-179	-179	1	179	179
ΔE (kcal/mol)	0	0.11	0.09	0.1	0.33	0.36
pop (%)	16	13	14	14	9	9
ΔG (kcal/mol)	0	0.06	0.12	0.18	0.50	0.53
Pop.(%)	18	16	15	13	8	7

<i>Vacuo</i>	G	H	I	J	K	L
H ₁ C ₁ C ₂ O*	-65	-71	-161	-162	-154	-161
C ₁ C ₂ OH*	-67	64	-53	178	-177	56
C ₉ C ₈ O ₈ H*	-2	2	1	179	4	-2
ΔE (kcal/mol)	0.41	0.61	0.69	0.94	1.23	1.40
pop (%)	8	6	5	3	2	1
ΔG (kcal/mol)	0.58	0.60	0.92	1.02	1.37	1.50
Pop.(%)	7	6	4	3	2	1

* in degrees

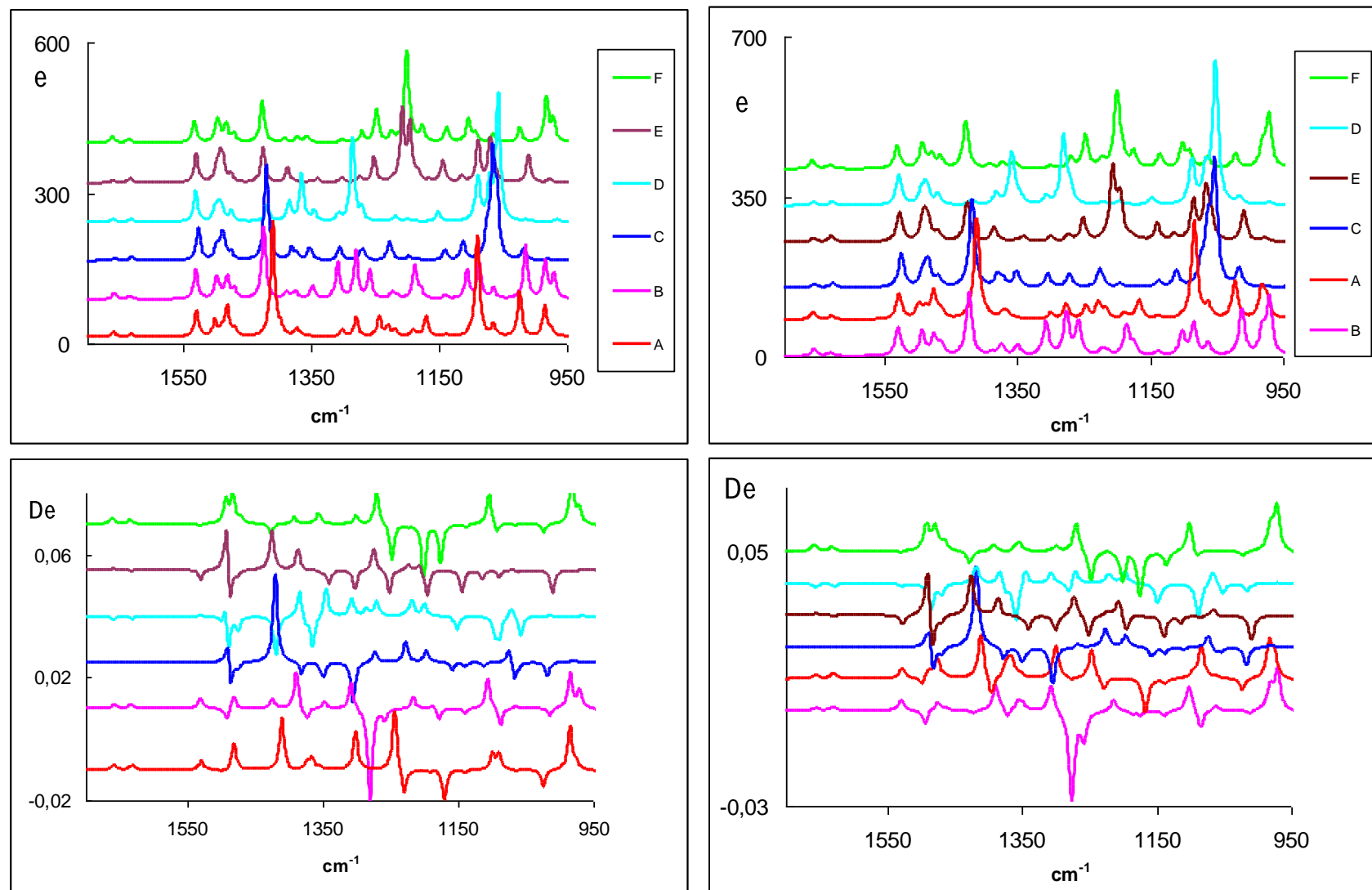
Fig.SI-9: B3PW91/TZ2P optimized structures and relative energies (kcal/mol) for (*R*)-1-aminotetralin (**1b**) *in vacuo*.



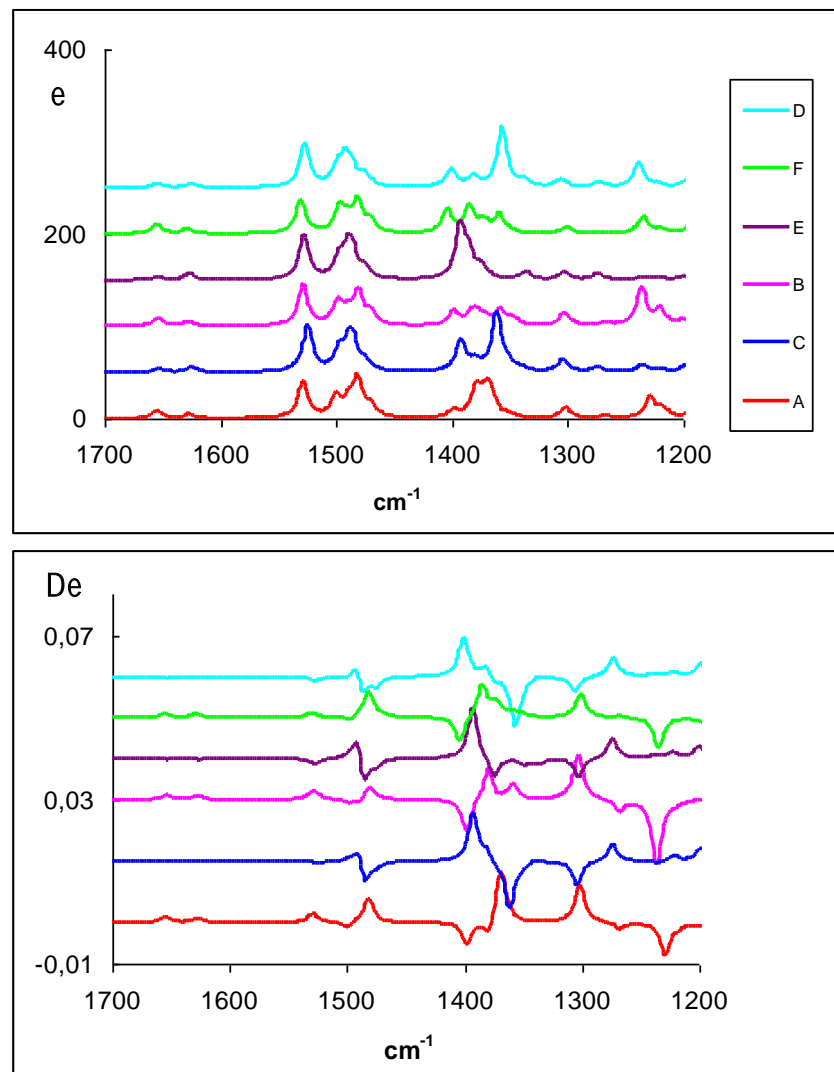
Vacuo	A	B	C	D	E	F
H ₂ C ₂ C ₁ N*	63	162	167	62	161	68
C ₉ C ₁ NH*	175	-55	45	-52	-59	62
C ₁ C ₉ C ₁₀ C ₄ *	-4	5	4	-2	2	-3
C ₂ C ₁ C ₉ C ₁₀ *	18	-21	-20	15	-15	16
C ₉ C ₁₀ C ₄ C ₃ *	18	-18	-17	19	-19	20
C ₄ C ₃ C ₂ C ₁ *	-48	-63	-63	64	-64	64
C ₁₀ C ₄ C ₃ C ₂ *	-47	46	46	-49	49	-49
C ₃ C ₂ C ₁ C ₉ *	-48	49	49	-46	46	-46
ΔE (kcal/mol)	0	0.30	0.28	0.54	0.53	1.86
pop (%)	32	20	20	13	13	1
ΔG (kcal/mol)	0	0.17	0.23	0.35	0.35	1.20
Pop.(%)	27	21	18	15	15	4

* in degree

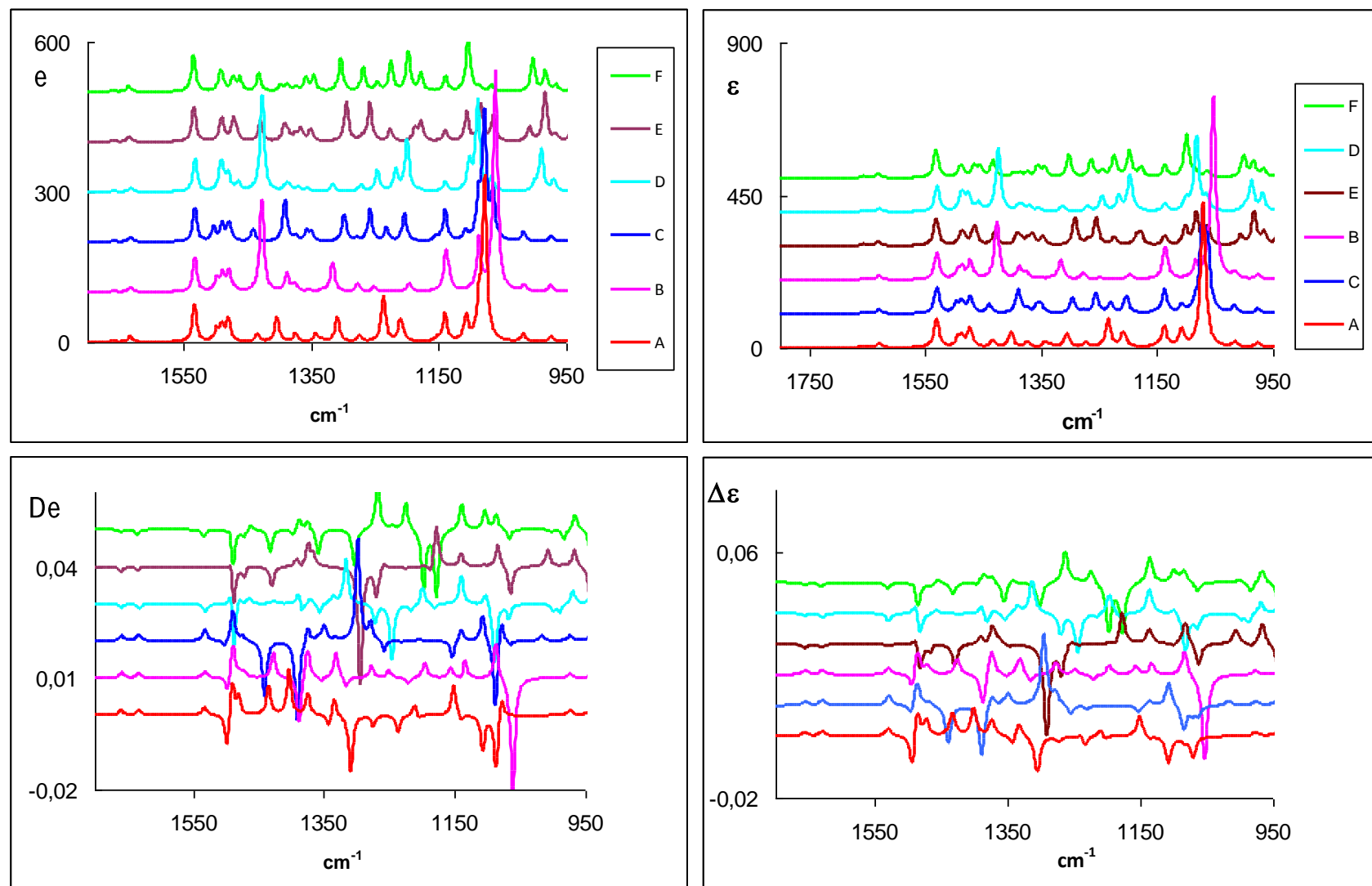
FigSI-10a: Calculated IR (top) and VCD (bottom) spectra of stable conformers of (*R*)-1-tetralol (**1a**) in *vacuo* (left) and in chloroform (right) with IEF-PCM method (B3PW91/TZ2P).



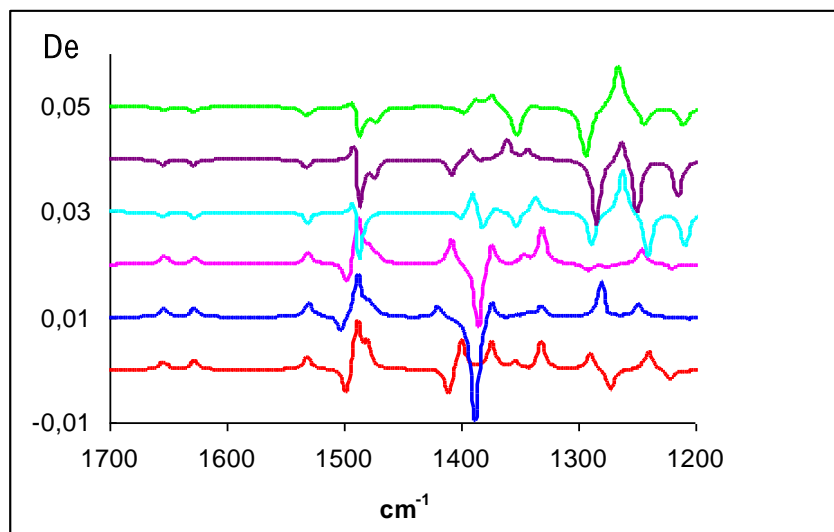
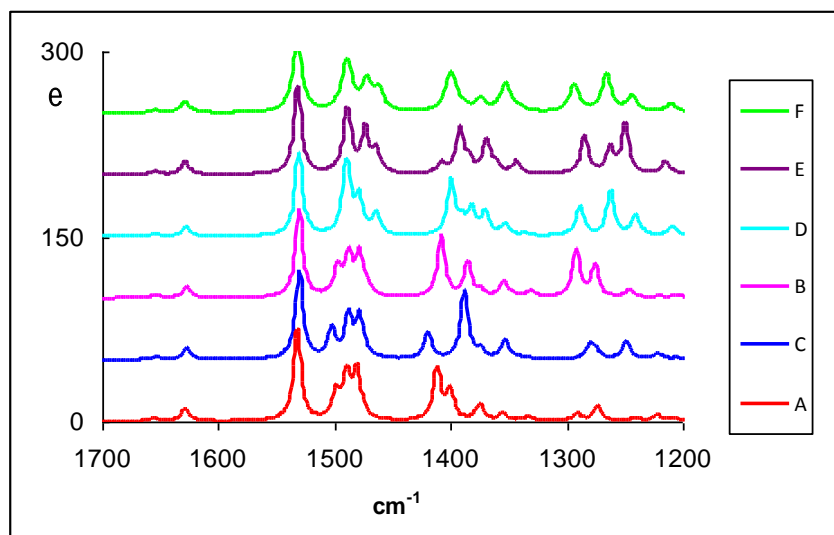
FigSI-10b: Calculated IR (top) and VCD (bottom) spectra of stable conformers of (*R*)-1-tetralol (**1a**) in methanol with IEF-PCM method(B3PW91/TZ2P)



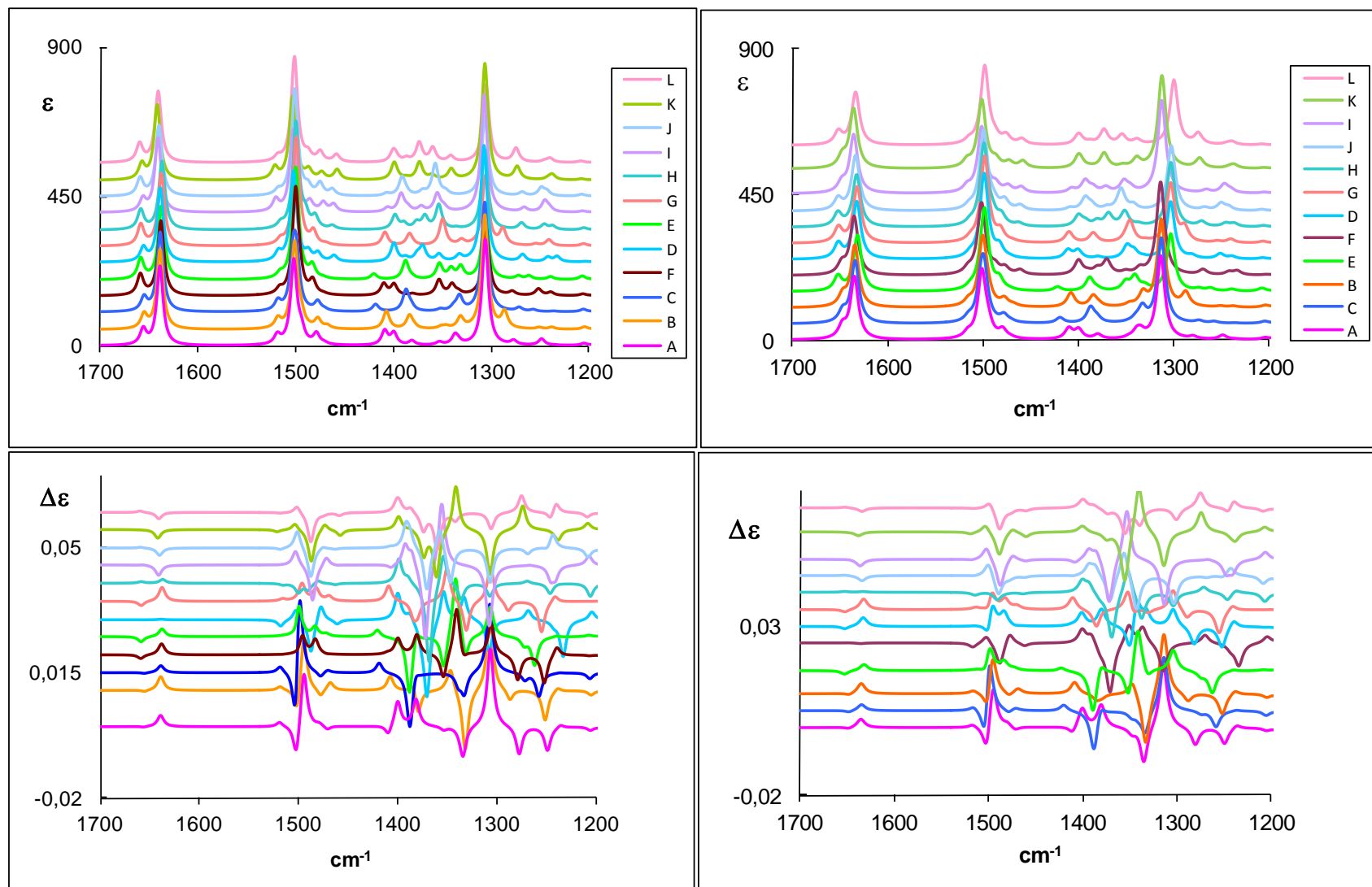
FigSI-11a: Calculated IR (top) and VCD (bottom) spectra of stable conformers of (*R*)-2-tetralol (**2a**) in *vacuo* (left) and in chloroform (right) with IEF-PCM method(B3PW91/TZ2P).



FigSI-11b: Calculated IR (top) and VCD (bottom) spectra of stable conformers of (*R*)-2-tetralol (**2a**) in methanol with IEF-PCM method(B3PW91/TZ2P).



FigSI-12: Calculated IR (top) and VCD (bottom) spectra of stable conformers of (*R*)-5-hydroxy-2-tetralol (**2b**) in *vacuo* (left) and in methanol (right) with IEF-PCM method(B3PW91/TZ2P).



FigSI-13: Calculated IR (top) and VCD (bottom) spectra of stable conformers of (*R*)-8-hydroxy-2-tetralol (**2c**) in *vacuo* (left) and in methanol (right) with IEF-PCM method(B3PW91/TZ2P).

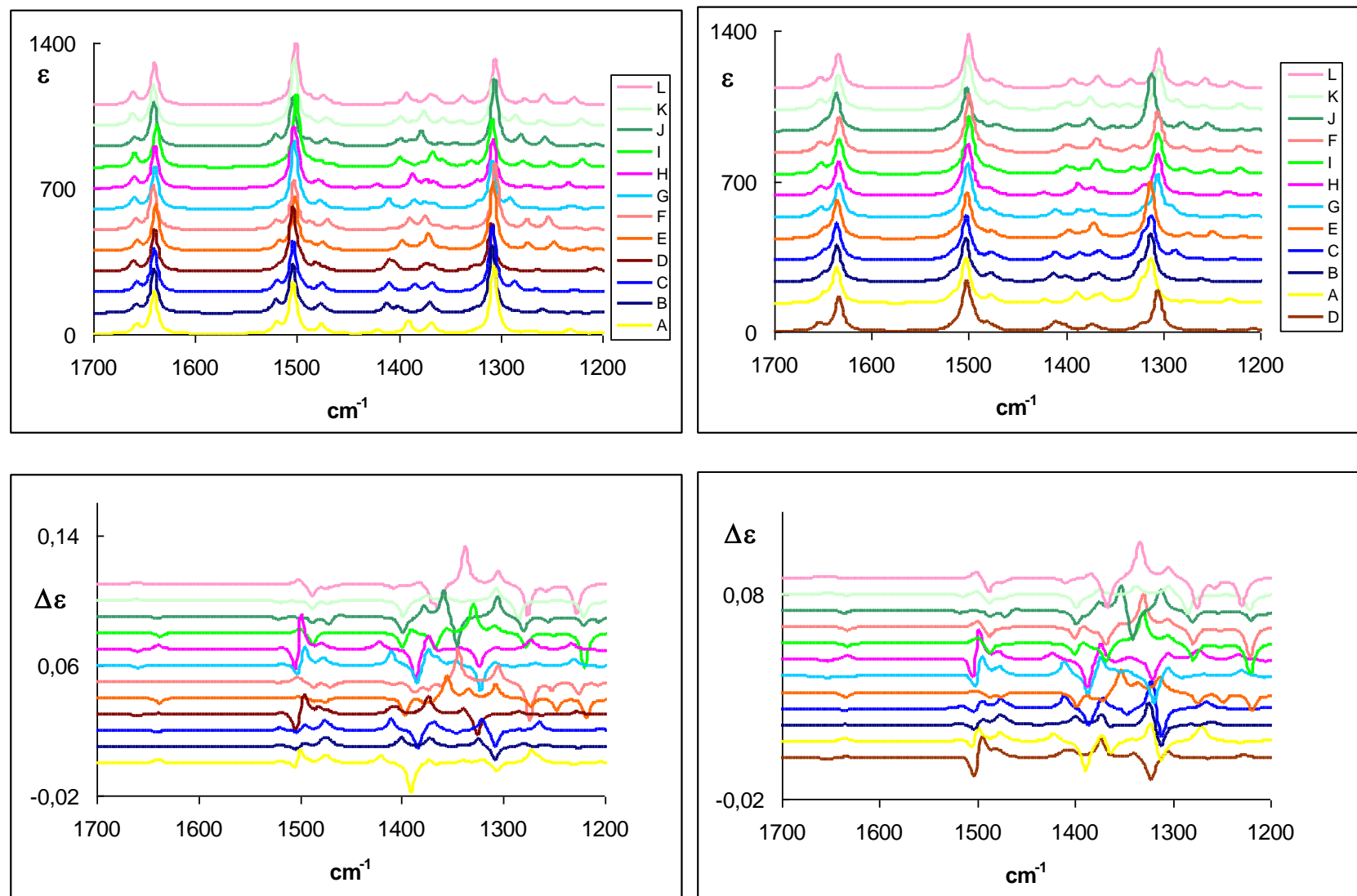


Fig.SI-14: Calculated IR (top) and VCD (bottom) spectra of stable conformers of (*R*)-1-aminotetralin (**1b**) in *vacuo*(B3PW91/TZ2P).

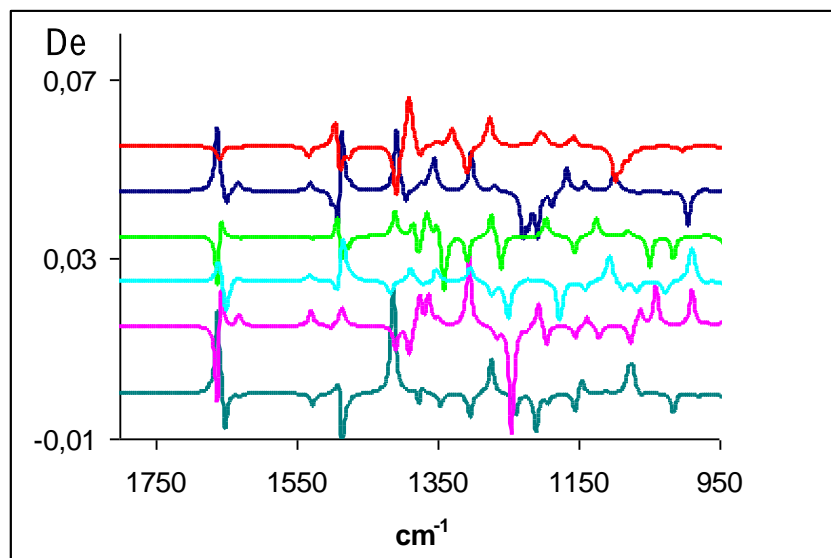
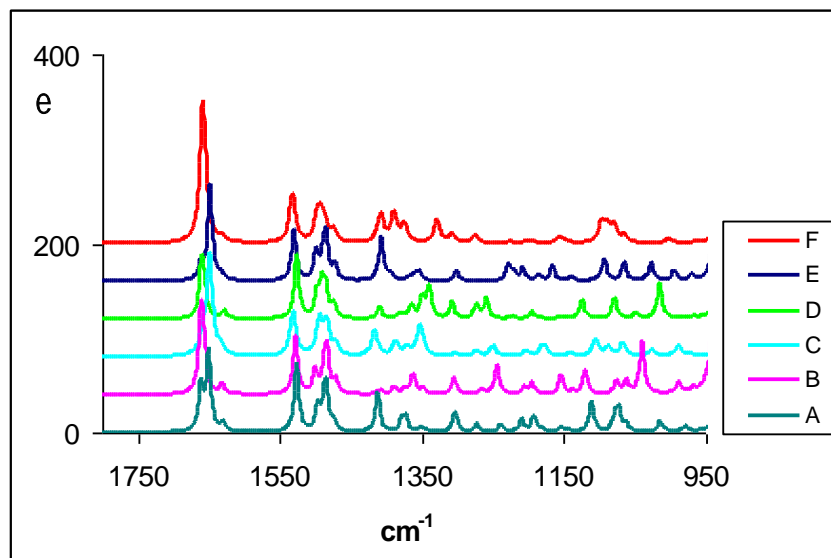


Fig. SI-15: Calculated absorption and ECD spectra of (*R*)-1-tetralol (**1a**) on the left and (*R*)-2-tetralol (**2a**) on the right with stable conformers (top) and weighted sum (bottom)

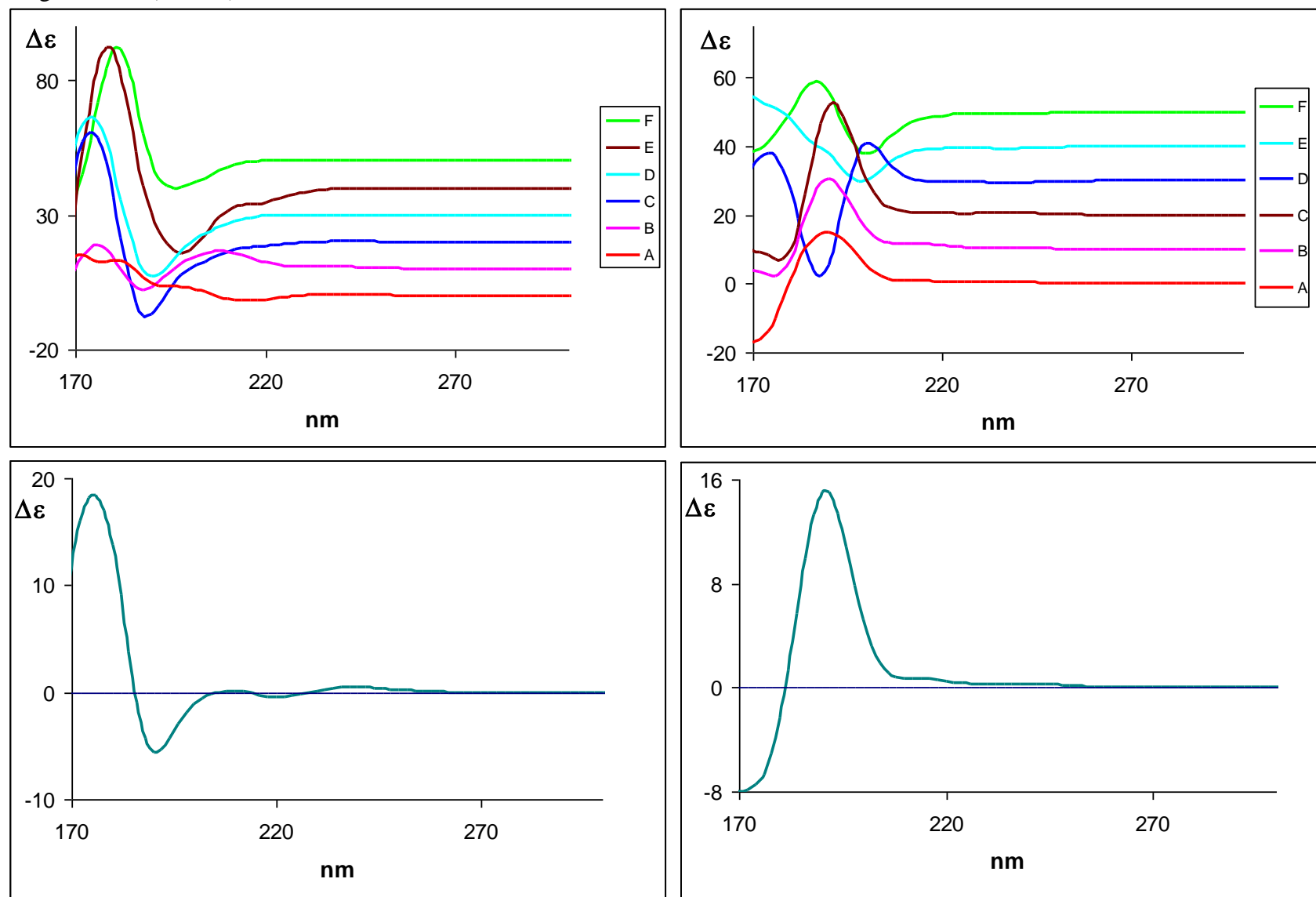


Fig. SI-16: Calculated absorption and ECD spectra of (*R*)-5-hydroxy-2-tetralol (**2b**) on the left and (*R*)-8-hydroxy-2-tetralol (**2c**) on the right with stable conformers (top) and weighted sum (bottom)

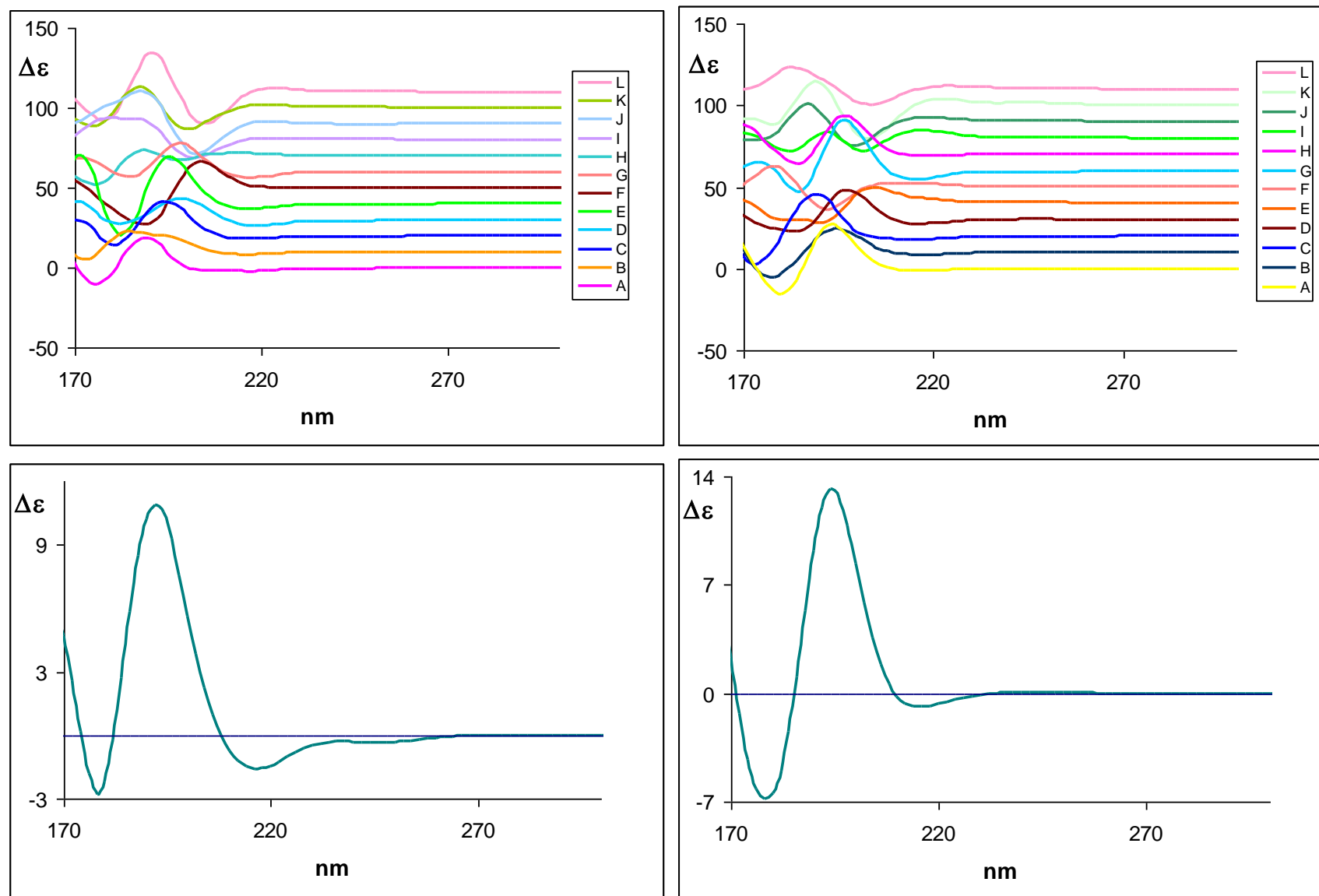


Fig. SI-17: Calculated absorption and ECD spectra of (*R*)-1-aminotetralin (**1b**) with stable conformers (top) and weighted sum (bottom) using B3LYP-TZVP.

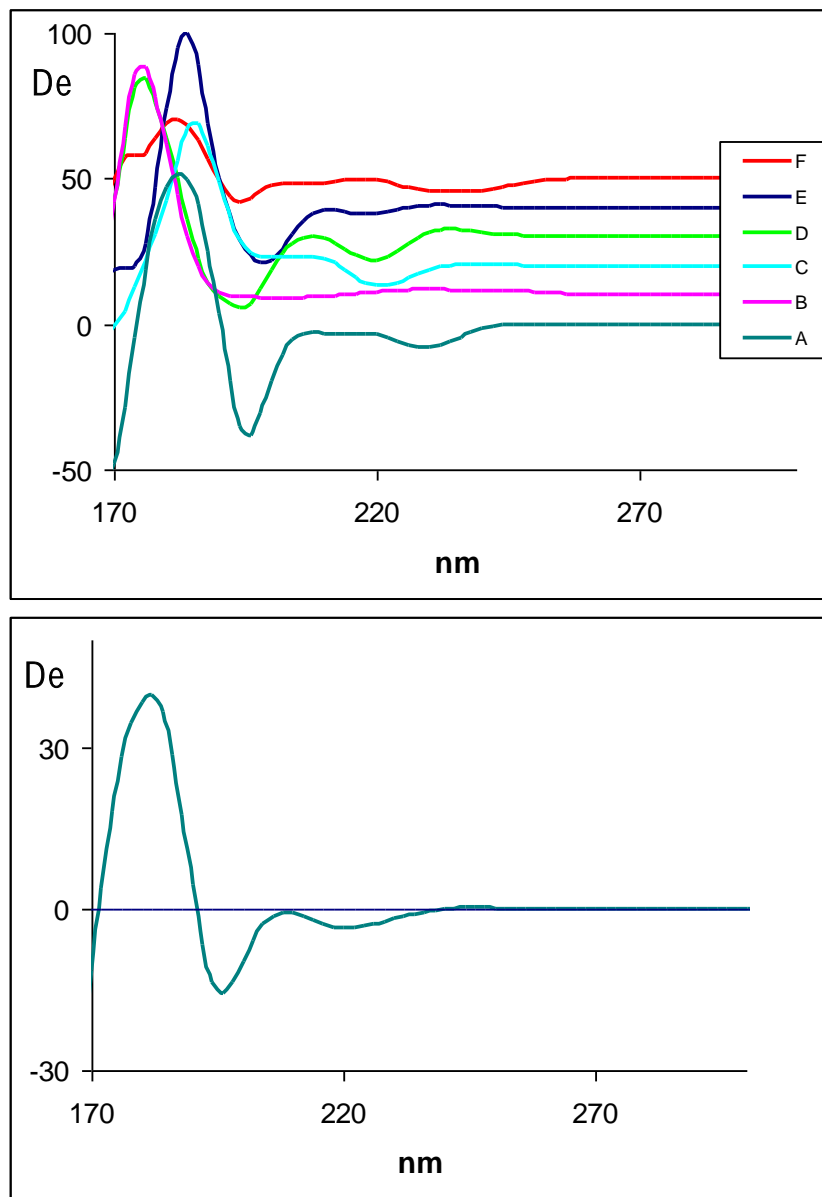
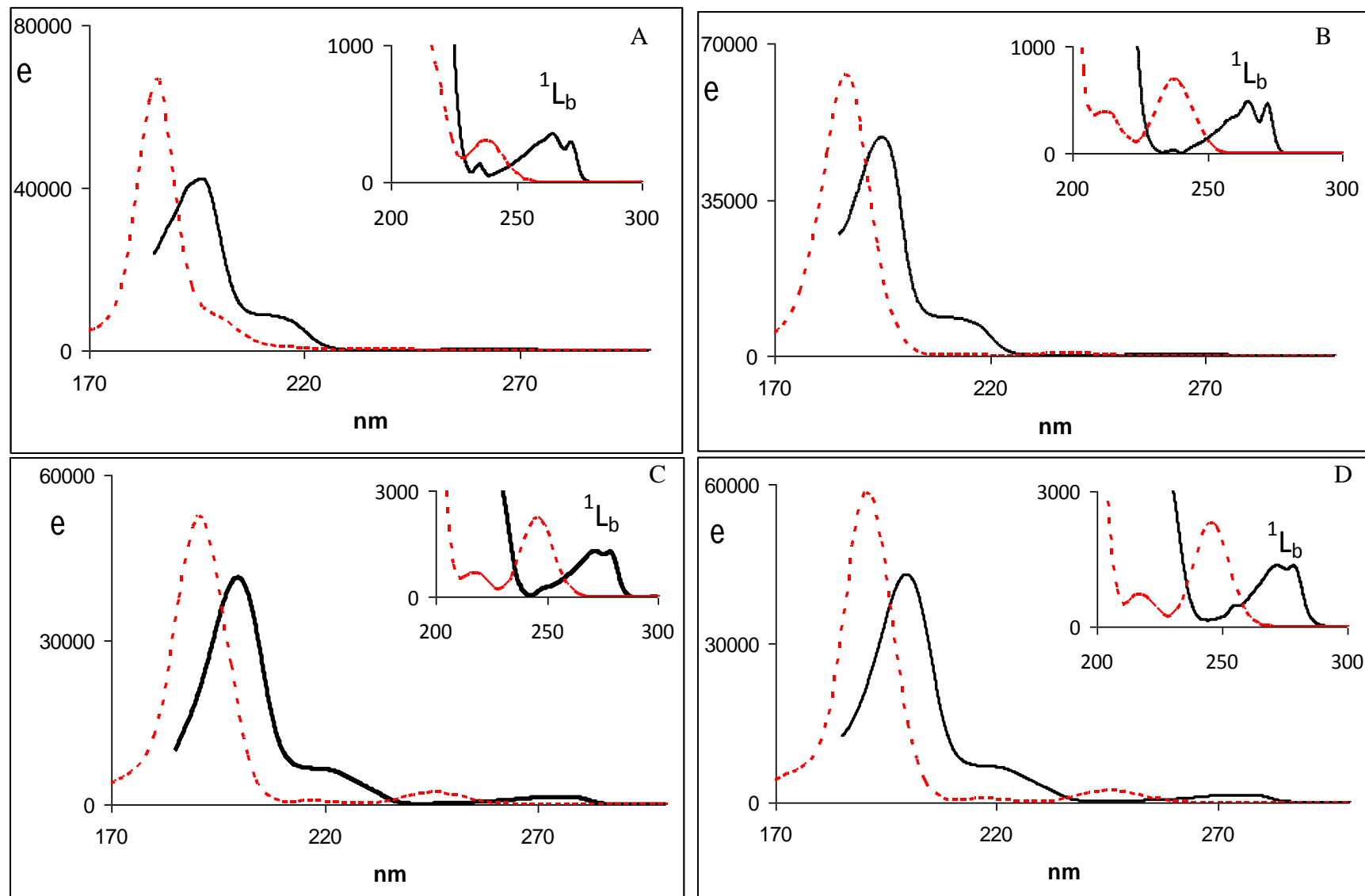


Fig. SI-18: Experimental (solid line) and calculated (dashed line) UV absorption spectra of (*R*)-1-tetralol (**A**), (*R*)-2-tetralol (**B**); (*R*)-5-hydroxy-2-tetralol (**C**), (*R*)-8-hydroxy-2-tetralol (**D**) and (*R*)-1-aminotetralin (**E**)



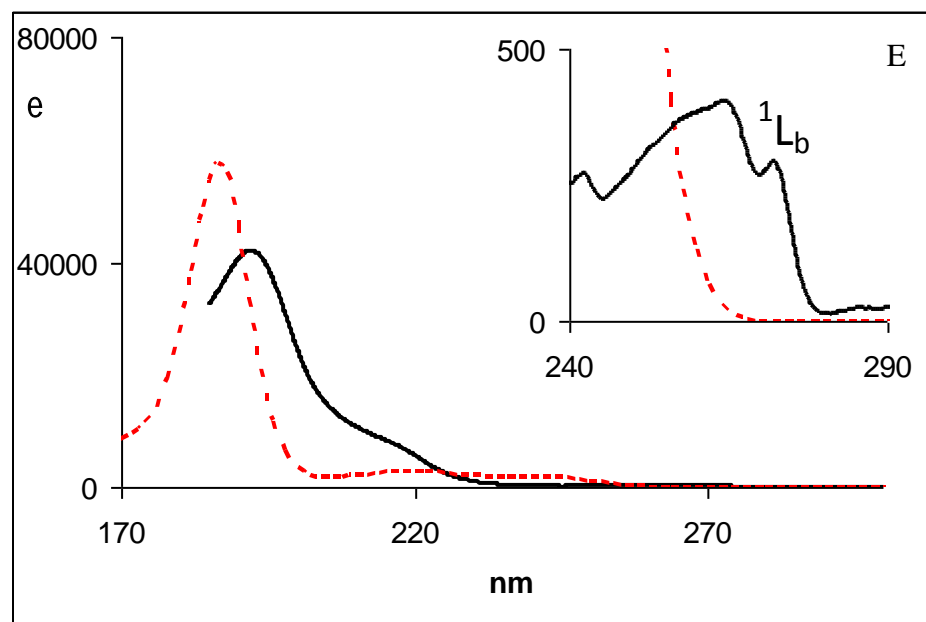


Table SI-1: Calculated conformer population factors (%) based on ΔG for (*R*)-1-tetralol (**1a**) and (*R*)-2-tetralol (**2a**) using B3PW91/TZ2P and B97D/TZ2P levels of theory within the PCM-CHCl₃ model.

1a	B3PW91-TZ2P (%)* PCM-CHCl ₃	B97D-TZ2P (%)* PCM-CHCl ₃
A	25	35
B	26	28
C	23	21
D	9	3
E	9	4
F	8	8

2a	B3PW91-TZ2P (%)* PCM-CHCl ₃	B97D-TZ2P (%)* PCM-CHCl ₃
A	31	21
B	24	27
C	25	19
D	7	19
E	7	8
F	6	7

- % population as determined from the ΔG calculations

Fig. SI-19a: : Experimental and calculated (weighted sum) IR (top) and VCD (bottom) spectra of (*R*)-1-tetralol (left panels) (**1a**) and (*R*)-2-tetralol (right panels) (**2a**) with B3PW91 (pink) and B97D (green) functionals with IEF-PCM (CHCl₃) method. The calculated IR and VCD spectra with B3PW91 functional using the population factor extracted from B97D calculations have been presented in blu.

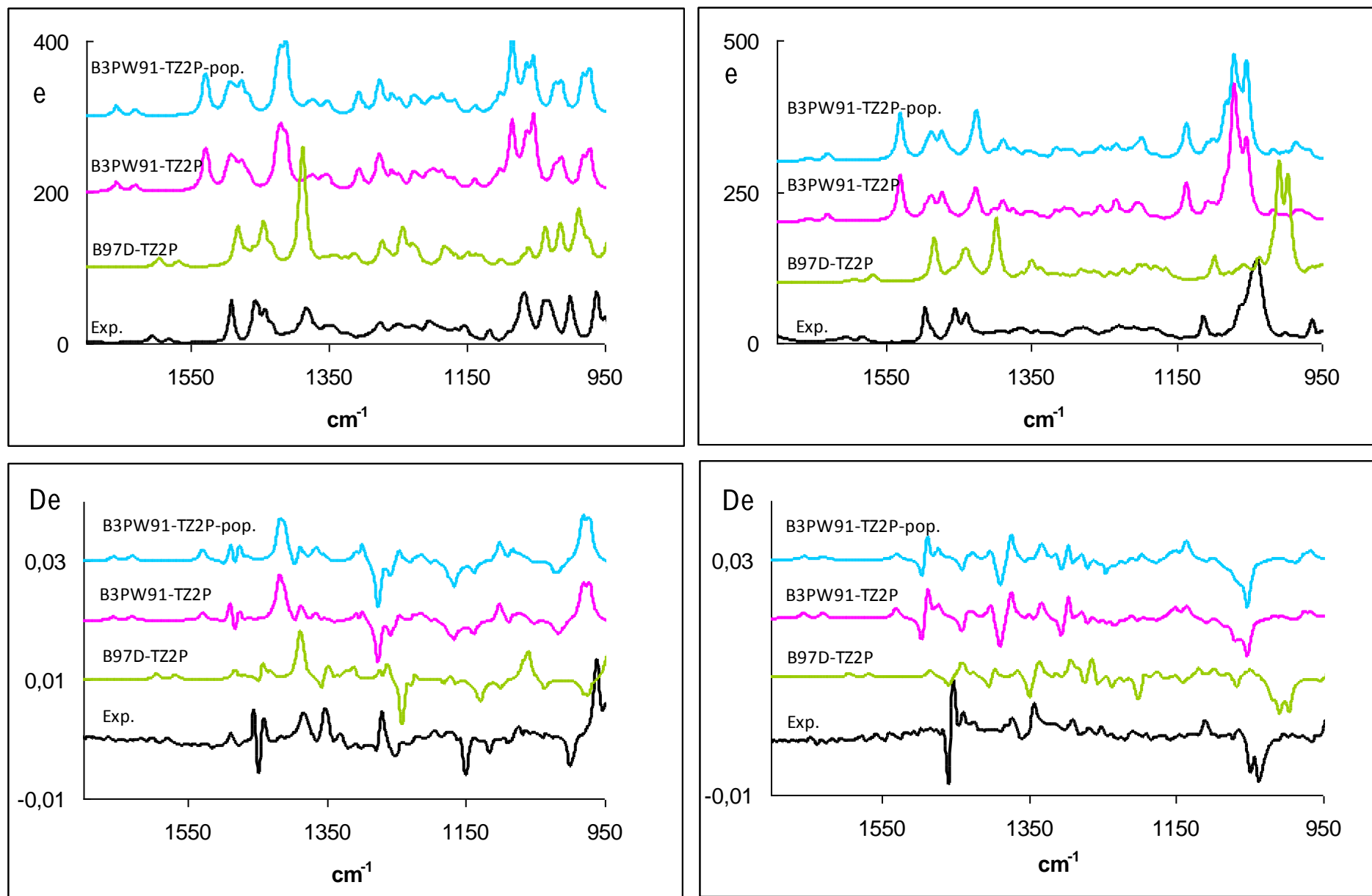


Fig. 19b. Calculated IR (top) and VCD (bottom) spectra for the six stable conformers of (*R*)-1-tetralol (left panels) (**1a**) and (*R*)-2-tetralol (right panels) (**2a**) on the basis of B97D/TZ2P level of theory for the PCM-CHCl₃ model.

